An EPR Study of Some Highly Distorted Tetrahedral Manganese(II) Complexes at High Magnetic Fields

Richard M. Wood,[1a] Debra M. Stucker,[1b] Laura M. Jones,[1a] W. Bryan Lynch,*,[1a] Sushil K. Misra,[1c] and Jack H. Freed[1d]

Department of Chemistry, University of Evansville, Evansville, Indiana 47722, Department of Chemistry, Gettysburg College, Gettysburg, Pennsylvania 17722, Department of Physics, Concordia University, Montreal, Quebec H3G 1M8, Canada, and Baker Laboratory of Chemistry, Cornell University, Ithaca, New York 14853

Received April 7, 1999

EPR spectra at 94.5 GHz (3 mm) and 249.9 GHz (1 mm) have been measured for the dichloro-, dibromo-, and diiodobis(triphenylphosphine oxide)manganese(II) complexes. These compounds have a distorted tetrahedral geometry, and the highest possible symmetry obtainable is C_{2v}. Because the spectra are taken in the high-field limit, they are simple and much easier to interpret than at lower magnetic fields. Accurate values of the zero-field splitting parameters, D and η (E/D), are determined by least-squares fitting and homotopy using matrix diagonalization. The compounds have g-values near 2 and large values of D and η. Across the series, D increases from 0.165 to 0.906 cm^{-1}, while η decreases slightly from 0.273 to 0.246.

Introduction

We are currently using EPR at high magnetic fields to examine a series of manganese-containing inorganic complexes in which the manganese(II) ion is in the high-spin state. Manganese complexes show a wide variety of bonding geometries, and EPR spectroscopy has been used successfully to probe the structures of these compounds.[2−7] The vast majority of the past work has been performed at lower magnetic fields (X- and Q-band). However, with samples of relatively large zero-field splitting (zfs), low-field EPR spectra are usually complicated, making analysis difficult.[8] We have found that a high-field EPR study results in fairly simple spectra that are much easier to interpret in terms of the axial (D) and rhombic (E) distortion parameters.[9]

We have already studied[9] two series of distorted octahedral manganese(II) complexes in which two of the ligand positions are occupied by halide ions. The Mn(4-picoline)$_4$X$_2$ compounds (X = Cl$^-$, Br$^-$, or I$^-$) were found to be axial with $\eta \approx 0$. ($\eta = E/D$ and may have values from zero to 1/3.) The Mn(*o*-phenanthroline)$_2$X$_2$ complexes have smaller D values than the picoline series. The lower values are most likely due to the cis arrangement of their halide ions[10−12] vs the trans arrangement of the picoline series, and not the ligand field strength of phenanthroline as was suggested in our earlier report.[9] A range of η values from 0.04 (dichloro) to 0.25 (diiodo) was found for the phenanthroline series; however, high values of η were determined for all three dihalo compounds in an earlier study at low magnetic fields.[10]

Here we examine a similar series in which the manganese(II) ion is bound in a distorted tetrahedral environment. The compounds are dichloro-, dibromo-, and diiodobis(triphenylphosphine oxide)manganese(II). The highest possible symmetry is C_{2v}, and these compounds are expected to have a large rhombic distortion, giving rise to large η values. This has been observed in EPR studies at low magnetic fields.[13−15]

We find that the high-field spectra of the tetrahedral compounds are simple and easy to interpret, and rough estimates of D and η can be made directly from the spectra. Accurate values of the zfs parameters can be determined by computer simulation, and we describe a technique that uses least-squares fitting and homotopy in conjunction with matrix diagonalization. This technique is especially important for the diiodo compound, where the value of D approaches 1 cm^{-1}. We find that third-order perturbation theory[9] does not provide a good overall fit of the experimental spectrum for such a high value of D, and an exact calculation of the spectrum was needed. Finally, we

(1) (a) University of Evansville. (b) Gettysburg College. (c) Concordia University. (d) Cornell University.

(2) Misra, S. K.; Sun, J.-S. *Magn. Reson. Rev.* **1991**, *16*, 57.
(3) Reed, G. H.; Markham, G. D. In *Biological Magnetic Resonance*; Berliner, L. J., Reuben, J., Eds.; Plenum: New York, 1984; Vol. 6, pp 73−142.
(4) Luck, R.; Stosser, R.; Poluektov, O. G.; Grinberg, O. Ya.; Lebedev, Ya. S. *Z. Anorg. Allg. Chem.* **1992**, *607*, 183.
(5) Xu, Y.; Chen, Y.; Ishizu, K.; Li, Y. *Appl. Magn. Reson.* **1990**, *1*, 283.
(6) Woltermann, G. M.; Wasson, J. R. *Inorg. Chem.* **1973**, *12*, 2366.
(7) Meirovitch, E.; Poupko, R. *J. Phys. Chem.* **1978**, *82*, 1920.
(8) Dowsing, R. D.; Gibson, J. F. *J. Chem. Phys.* **1969**, *50*, 294.
(9) Lynch, W. B.; Boorse, R. S.; Freed, J. H. *J. Am. Chem. Soc.* **1993**, *115*, 10909.
(10) Dowsing, R. D.; Gibson, J. F.; Goodgame, M.; Hayward, P. J. *J. Chem. Soc. A* **1970**, 1133.
(11) (a) Ballhausen, C. J. *Introduction to Ligand Field Theory*; McGraw-Hill: New York, 1962; pp 106−108. (b) Heming, M.; Remme, S.; Lehmann, G. *J. Magn. Reson.* **1986**, *69*, 134.
(12) (a) McKenzie, E. D. *Coord. Chem. Rev.* **1971**, *6*, 187. (b) Morcom, R. E.; Bell, C. F. *J. Inorg. Nucl. Chem.* **1973**, *35*, 1865. (c) Malinowski, T. J.; Kravtsov, V. Ch.; Simonov, Y. A.; Lipkowski, J.; Bologa, O. A. *J. Coord. Chem.* **1996**, *37*, 187. (d) Zhou, K.-J.; Zhang, C.-G.; Xu, D.-J.; Xu, Y.-Z. *Jiegou Huaxue* **1997**, *16*, 20. (e) McCann, S.; McCann, M.; Casey, M. T.; Jackman, M.; Devereux, M.; McKee, V. *Inorg. Chim. Acta* **1998**, *279*, 24.
(13) Dowsing, R. D.; Gibson, J. F.; Goodgame, D. M. L.; Goodgame, M.; Hayward, P. J. *J. Chem. Soc. A* **1969**, 1242.
(14) Vivien, D.; Gibson, J. F. *J. Chem. Soc., Faraday Trans. 2* **1975**, *71*, 1640.
(15) Kosky, C. A.; Gayda, J.-P.; Gibson, J. F.; Jones, S. F.; Williams, D. J. *Inorg. Chem.* **1982**, *21*, 3173.

10.1021/ic990377+ CCC: $18.00 © 1999 American Chemical Society
Published on Web 11/15/1999

will show that, for these samples, the value of η decreases slightly as we go from the dichloro to the diiodo compound.

Experimental Section

The tetrahedral complexes were prepared in absolute ethanol as described earlier.[16] Our best spectra (those relatively free of impurity signals) were produced from dichloro and diiodo samples prepared at or near room temperature and dibromo samples prepared at 45 °C. The diiodo complex was made and stored in the dark to prevent the formation of iodine.

All samples were studied as neat powders. X-band spectra (not shown) were taken with a Varian E-4 spectrometer. Two different high-field EPR spectrometers were used. Spectra of the dichloro compound were taken at 3 mm (94.5 GHz) with the high-field instrument at the Illinois EPR Research Center (IERC). This instrument uses a cylindrical cavity and has been described elsewhere.[17] The 3 mm spectra presented here are the average of eight individual scans. Spectra at 1 mm (249.9 GHz) were taken at Cornell University. The 1 mm instrument uses a transmission Fabry−Perot cavity and has also been described elsewhere.[9,18] The temperature of the samples was between 0 and 20 °C. Field modulation was usually 1−5 G at approximately 100 kHz. The accuracy with which the field value can be determined for both high-field instruments is better than ±10 G, when the main magnet coil is swept.

The dichloro compound was studied at 3 mm because its full spectrum could be observed with the 3 mm instrument, and it is already in the high-field limit. Also, a significant distortion in the $g = 2$ line due to dispersion was present at 1 mm. Much smaller amounts of dispersion were present in the dibromo and diiodo spectra, and these were corrected by standard methods.[19] The spectra of all three samples were corrected for any baseline drift.

Initial estimates for the parameters g, D, and E, and the line width were made with a field-swept EPR simulation program using third-order perturbation theory and running on a desktop computer.[7,9] (The relevant equations in ref 9 contain a number of errors; see ref 20 for the correct perturbation expressions.) These values served as initial parameters in a least-squares fitting (LSF) program using the technique of homotopy in conjunction with matrix diagonalization (HTMD),[21,22] which has recently been developed for powder spectra from transition metal ions. Details of the HTMD technique are briefly summarized in the Appendix. We considered both Lorentzian and Gaussian line shapes, and we found that the latter yielded significantly better fits, although comparable g, D, and E values were obtained using either line shape.

Results

High-field spectra of all three tetrahedral compounds are shown in Figure 1. Field values for the 1 mm spectra (dibromo and diiodo samples) are given on the lower axis; field values at 3 mm (dichloro sample) are shown on the top axis. Note the large signal intensity at $g = 2$ (approximately 34 and 89 kG) and the presence of lines at lower fields. For the dibromo and diiodo samples there are lines at much higher fields, but the maximum magnetic field strength of the 1 mm instrument (95 kG at 4.2 K) prevents their observation. Because of the relatively large line widths, the manganese nuclear hyperfine splitting is not observed. The g values and the zero-field splitting parameters were determined by least-squares fitting of the experimental spectra using the HTMD technique. These values are summarized in Table 1. The fits for all three compounds are shown as dotted curves in Figures 3−5. The g values for the samples are very close to 2.0, which is typical of the high-spin manganese(II) ion. The estimated standard deviations provided by the least-squares fitting are very small (±5 G or less), so the errors in g, D, and E (and hence η) reported in Table 1 are based primarily upon the accuracy to which the magnetic field value can be determined.

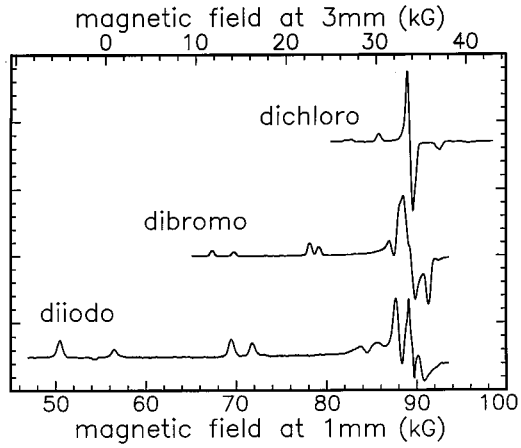

Figure 1. High-field EPR spectra of dichloro-, dibromo-, and diiodobis(triphenylphosphine oxide)manganese(II) complexes. The dichloro spectrum was taken at 3 mm (top horizontal axis), and the dibromo and diiodo spectra were taken at 1 mm (lower horizontal axis).

Discussion

The high-field EPR spectra of manganese(II) complexes with large rhombic distortions can be understood with the help of Figure 2. This figure gives first-order line positions, relative to $g = 2$, for manganese(II) EPR spectra in the high-field limit and for varying values of η. It also gives the electron spin assignments, for positive values of D and E, for many of the transitions. The manganese spectrum is, to first-order, symmetrical about $g = 2$. For axially distorted spectra ($\eta = 0$), there are three lines downfield and three upfield from $g = 2$. The positions of the lines are determined by the size of D, the outer lines of the spectrum being $4D$ removed from $g = 2$. As the rhombic distortion increases toward its maximum value ($\eta = 1/3$), the three overlapping transitions at $\pm 2D$ split into three single lines and the two transitions initially at $\pm D$ split into two single lines. The positions of these lines are dependent upon the size of η. At the maximum value of η, there are only two lines downfield and two upfield from $g = 2$, each composed of two overlapping transitions. The line at $\pm D$ is lost. In particular, as η increases from 0 to 1/3, the $-3/2 \leftrightarrow -5/2$ (y) transition shifts from $-2D$ toward the $5/2 \leftrightarrow 3/2$ (z) transition, which is independent of η and located at $-4D$. The nearer η is to its maximum value, the closer these lines are to one another. The $-1/2 \leftrightarrow -3/2$ (y) transition (originally at $-D$) also moves downfield as η increases. It will eventually join the $3/2 \leftrightarrow 1/2$ (z) transition, whose position is independent of η and located at $-2D$. For a given value of η, the splitting in the pair of lines near $-4D$ is always larger than that at $-2D$. Similar statements can be made for transitions upfield from $g = 2$.

Comparing Figures 1 and 2, we see that the dichloro compound has a single, strong line at $g = 2$. For the dibromo and diiodo compounds, there are many lines near $g = 2$ that arise from higher-order splittings in the $+1/2 \leftrightarrow -1/2$ transition (not shown in Figure 2) that appear at high values of D. Some of the lines are also due to η-dependent transitions from the

(16) Goodgame, D. M. L.; Cotton, F. A. *J. Chem. Soc.* **1961**, 3735.
(17) Smirnova, T. I.; Smirnov, A. I.; Belford, R. L.; Clarkson, R. B. *J. Am. Chem. Soc.* **1998**, *120*, 5060.
(18) Lynch, W. B.; Earle, K. A.; Freed, J. H. *Rev. Sci. Instrum.* **1988**, *59*, 1345.
(19) Earl, K. A.; Budil, D. E.; Freed, J. H. *J. Phys. Chem.* **1993**, *97*, 13289.
(20) Misra, S. K. *Physica* **1997**, *B240*, 183.
(21) Misra, S. K. *J. Magn. Reson.* **1999**, *137*, 83.
(22) Misra, S. K. *J. Magn. Reson.* **1999**, *140*, 179.

Table 1. Results of High-Field EPR of Tetrahedral Mn(triphenylphosphine oxide)$_2$X$_2$ Compounds

halide, X	g value	D (cm^{-1})	E (cm^{-1})	η	width (G)
Cl	2.0000 ± 0.0006	0.165 ± 0.001	0.045 ± 0.001	0.273 ± 0.006	316
Br	1.9985 ± 0.0003	0.507 ± 0.001	0.134 ± 0.001	0.263 ± 0.002	393
I	2.0039 ± 0.0003	0.906 ± 0.001	0.223 ± 0.001	0.246 ± 0.001	518

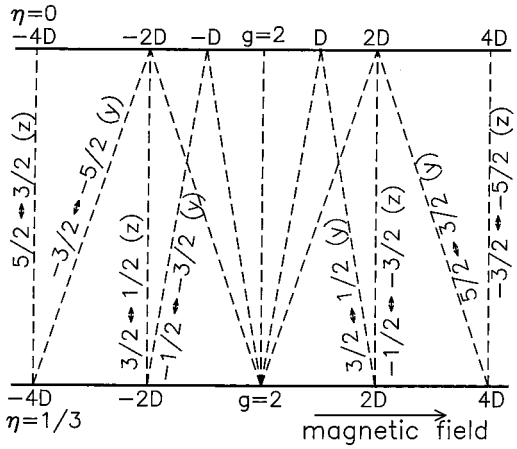

Figure 2. Schematic diagram of the first-order predictions for manganese(II) EPR as a function of η in the high-field limit. Magnetic field positions of the transitions are shown relative to the $g = 2$ field value. Assignments (see ref 9) for the eight outer transitions are given for positive values of D and E. Transitions that converge at $g = 2$ when $\eta = 1/3$ are, in order of increasing magnetic field, $-3/2 \leftrightarrow -5/2$ (x), $-1/2 \leftrightarrow -3/2$ (x), $1/2 \leftrightarrow -1/2$ (x,y,z), $3/2 \leftrightarrow 1/2$ (x), and $5/2 \leftrightarrow 3/2$ (x).

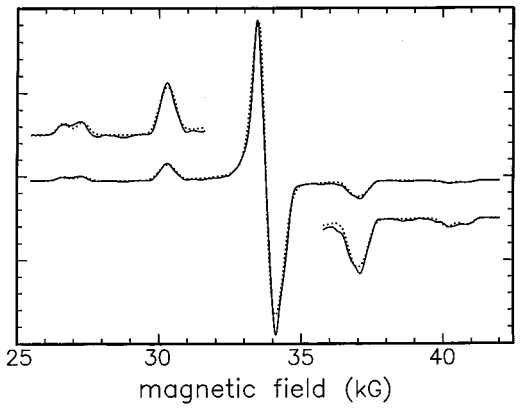

Figure 3. EPR (3 mm) of Mn(triphenylphosphine oxide)$_2$Cl$_2$ (—) with simulation (···) using $g = 2.0000$, $D = 0.165$ cm^{-1}, $\eta = 0.273$, and line width 316 G.

$\pm 2D$ and $\pm D$ positions that merge near $g = 2$ at high values of η. Only the complete spectrum of the dichloro compound was observed; much of the dibromo and diiodo spectra at fields higher than $g = 2$ could not be observed due to the limited maximum field strength of the 1 mm spectrometer. However, the position of the $-4D$ line for all three compounds clearly shows that D is largest for the diiodo compound, and smallest for the dichloro compound. All three spectra are similar to Figure 2 if η is very near its maximum value, since none of the spectra show a line at $\pm D$, and we observe small splittings downfield from $g = 2$.

The dichloro spectrum taken at 3 mm, along with our best fit, can be seen in Figure 3. The splittings in the outer lines are the smallest of all three complexes, and the value of η is large enough that the $3/2 \leftrightarrow 1/2$ (z) and $-1/2 \leftrightarrow -3/2$ (y) transitions are unresolved at $-2D$. A similar statement can be made for the $+2D$ line. From our best fit (the dotted curve in Figure 3) we find that $D = 0.165$ cm^{-1} and $\eta = 0.273$. The outer regions

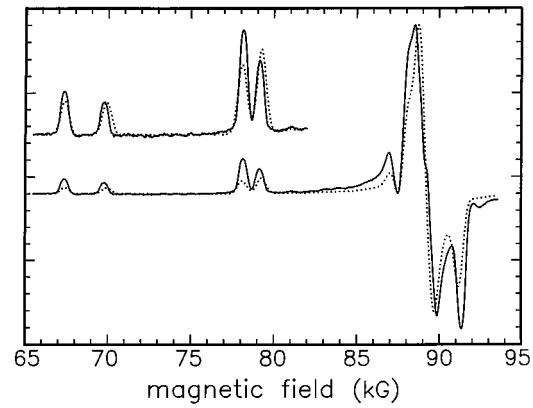

Figure 4. EPR (1 mm) of Mn(triphenylphosphine oxide)$_2$Br$_2$ (—) with simulation (···) using $g = 1.9985$, $D = 0.507$ cm^{-1}, $\eta = 0.263$, and line width 393 G. Intensities of the magnified region are normalized to the line at 69.9 kG.

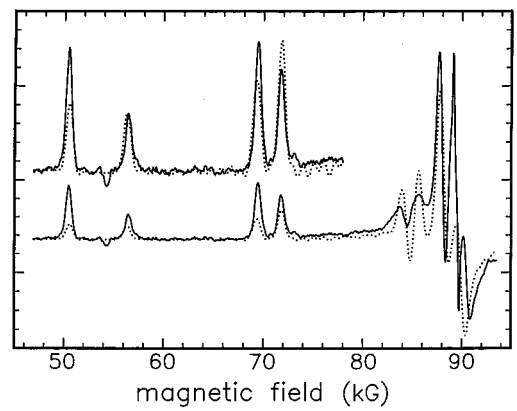

Figure 5. EPR (1 mm) of Mn(triphenylphosphine oxide)$_2$I$_2$ (—) with simulation (···) using $g = 2.0039$, $D = 0.906$ cm^{-1}, $\eta = 0.246$, and line width 518 G. Intensities of the magnified region are normalized to the line at 56.5 kG.

of the spectrum are magnified in Figure 3 so that the small splittings and their fit can be more easily observed.

The splittings in the lines downfield from $g = 2$ in the dibromo spectrum (Figure 4) are much larger than those in the dichloro spectrum, and the transitions near $-2D$ are now easily resolved. The size of these splittings will increase as D increases and/or the value of η decreases. We find that D is 0.507 cm^{-1}, and η is only 0.263, about 4% smaller than that of the dichloro sample. The fit of the dibromo spectrum (Figure 4) is very good, although the downfield lines are about twice as intense as predicted.

The spectrum of the diiodo compound, along with our simulation, is shown in Figure 5. The D value has now increased to 0.906 cm^{-1}, and we expect and observe even larger splittings in the pairs of lines downfield from $g = 2$. As with the dibromo sample, the splittings are too large to be caused by the higher D value alone, and η has decreased even further to 0.246. The fit of the diiodo spectrum is very good, although the intensities of the downfield lines, like those of the dibromo spectrum, are larger than predicted. Also, the negative line at 91 kG (a $+1/2 \leftrightarrow -1/2$ transition) is less intense than predicted and is about 500 G upfield from its expected position. We believe the lines

at 54 and 89.5 kG are caused by impurities of unknown origin. Matrix diagonalization was essential to accurately fit the diiodo spectrum, indicating that it is not quite in the high-field limit. At $g = 2$, the field value is only 9 times the value of D; at $-4D$, it is only $5D$. We found that approximate methods, in particular third-order perturbation theory,[9] cannot fit all regions of the spectrum simultaneously, (e.g., the $g = 2$ region vs the $-2D$ and $-4D$ regions).

Despite the difficulties in obtaining adequate fits by the more approximate methods, we thought it useful to compare the values of D and E obtained from HTMD and least-squares fitting with values estimated directly from the spectrum and by fitting with third-order perturbation theory (PT), according to some simple and well-defined procedure. Rough estimates of D and E can be obtained from various splittings in the spectrum, if we assume a first-order spectrum as in Figure 2. An approximate value for D can be obtained from half the splitting between the $-4D$ and $-2D$ lines. η can be approximated from the splitting, δ, between the two lowest-field lines in each spectrum, $5/2 \leftrightarrow 3/2$ (z) and $-3/2 \leftrightarrow -5/2$ (y), using the first-order equation, $\eta = 1/3 - \delta/(6D)$. From D and η, a value for E can be found. Values of D and E can also be determined with third-order PT using a field-swept program[9] and fitting by trial-and-error. In determining the best fit, more emphasis was given to fitting the $-2D$ and $-4D$ regions rather than the splittings at $g = 2$. We find there is reasonable agreement between the HTMD values and those estimated directly from the spectra and from PT according to the procedure described. Estimated values of D and E are within 9% of the HTMD values; values of D and E using PT are within 6% of the HTMD values. We believe the reasonable agreement of the three methods is due to the inherent simplicity of the high-field spectra. In practice then, good initial estimates of the zfs parameters may be found from preliminary fits using perturbation theory, and they may then be used to seed the LSF using HTMD to obtain accurate final values.

We find that D values for the tetrahedral compounds increase in the order $Cl^- < Br^- < I^-$, a trend found in many other manganese(II) halide complexes.[10,23,24] Also, the value of η decreases slightly, and this implies an increasing distortion from the tetrahedral arrangement across the dihalo series.[13]

This series of complexes has been studied previously at X- and Q-band as pure and dilute powders[13] and as single crystals[14,15] in which the manganese compound is doped into the corresponding dihalobis(triphenylphosphine oxide)zinc(II) compound. There is reasonable agreement between the zfs parameters determined from low- and high-field powder studies. D and η values differ by no more than 20%, except for the dichloro compound, where the D values differ by almost a factor of 2. This is probably due to the difficulty of assigning turning points in the low-field powder spectra.[15] When our high-field results are compared with the results from previous single-crystal work of the dichloro and dibromo compounds,[14,15] the agreement is much better; our values of D for the pure dichloro and dibromo powder samples are lower by only 0.007 and 0.016 cm^{-1}, respectively, compared to the doped single-crystal values. The even smaller differences in E values (no more than 0.002 cm^{-1}) are within experimental error. The slightly lower D values found in our work on pure powder samples are most likely caused by host effects. It has been shown[6,23,25] that, as the size of the host metal ion decreases, the D value for many manganese(II) complexes increases. Since the ionic radius of manganese(II) is larger[6] than that of zinc(II), it seems likely that this is the cause for the slightly lower D values observed in the pure powder samples.

Appendix

Evaluation of Spin-Hamiltonian Parameters and Line Widths by Least-Squares Fitting and Homotopy Using Matrix Diagonalization.[22] First, the polycrystalline EPR spectrum is simulated by the use of the HTMD technique.[21] This is accomplished by overlapping single-crystal spectra computed for a large number of uniformly distributed orientations (θ, φ) of **B** over the unit sphere weighted in proportions of $\sin\theta\, d\theta\, d\varphi$ to take into account the distribution of various constituting crystallites whose principal axes are oriented in the interval $d\theta$, $d\varphi$ about (θ, φ).

The simulated powder spectrum is expressed as discrete sums over uniformly distributed, infinitesimally close, orientations (θ, φ) of **B** over the unit sphere, as well as over infinitesimally close values of B, denoted as B_k, covering an appropriate range of B values, summing over all the transition lines for each chosen orientation of **B**, as follows:

$$S(B,\nu_c) = C \sum_{i,\theta_j,\varphi_j,k} P(i,\theta_j,\varphi_j,\nu_c)\, F(\omega_i, B_r(i,\theta_j,\varphi_j,\nu_c), B_k) \sin\theta_j \tag{1}$$

In eq 1, $P(i,\theta_j,\varphi_j,\nu_c)$ is the transition probability for the ith transition between the levels i' and i'' of the eigenpair in resonance at the microwave frequency ν_c at the orientation (θ, φ) of **B** over the unit sphere. The values of θ_j are distributed over the range 0 to $\pi/2$, while those of φ_j are distributed over 0 to 2π. The summation over k takes into account the probability of the amplitude of absorption at the magnetic field value B_k due to the line shape distribution $F(\omega_i, B_r(i, \theta_j, \varphi_j, \nu_c), B_k)$ for the ith transition for the orientation of **B** along the (θ_j, φ_j) direction.

The transition probability in eq 1 is given by

$$P(i,\theta,\varphi,\nu_c) \propto |\langle\Phi_{i'}|(B_{1x}S_x + B_{1y}S_y + B_{1z}S_z)|\Phi_{i''}\rangle|^2 \tag{2}$$

where S_α and $B_{1\alpha}$ ($\alpha = x, y, z$) represent the components of the electron spin operator, **S**, and the modulation radio-frequency field $\mathbf{B_1}$. $|\Phi_{i'}\rangle$ and $|\Phi_{i''}\rangle$ are the eigenvectors of the spin-Hamiltonian (SH) matrix corresponding to the energy levels $E_{i'}$ and $E_{i''}$ of the eigenpair in resonance. The same eigenpair in resonance consisting of energy levels characterized by the electronic magnetic quantum numbers M and $M - 1$, which describe the eigenvectors of H_{Ze}, the Zeeman part of the spin Hamiltonian, should be used for the calculation of the resonant fields corresponding to allowed fine-structure transitions as the orientation of **B** is changed in infinitesimally close steps to cover the unit sphere.[21] Otherwise, the satellite lines near the central Mn(II) transition are missed in particular. It is not straightforward to accomplish this, particularly when the orientation of the crystal axis is far away from that of the external magnetic field; the appropriate strategy is described in ref 21.

The absorption spectrum is then calculated by performing the sum in eq 1 with $P(i,\theta_j,\varphi_j)$ centered at $B_r(i,\theta_j,\varphi_j,\nu_c)$, referred to hereafter as B_{ri}, with the line shape function $F(B_{ri},B_k)$, which was chosen here to be Gaussian, extended over an appropriate magnetic-field interval $\pm\Delta B$ about B_{ri}, characteristic of the line shape:

$$F_G(B_{ri},B_k) = K_G \exp[-(B_k - B_{ri})^2/\sigma^2] \tag{3}$$

(23) Birdy, R. B.; Goodgame, M. *Inorg. Chim. Acta* **1981**, *50*, 183.
(24) Dowsing, R. D.; Gibson, J. F.; Goodgame, M.; Hayward, P. J. *J. Chem. Soc. A* **1969**, 187.
(25) Wolterman, G. M.; Wasson, J. R. *J. Phys. Chem.* **1973**, *77*, 945.

where B_{ri} is the resonant field value for the ith transition, σ is the line width, and K_G $\{=(1/B_\Delta)(\ln(2/\pi))^{1/2}\}$ is the normalization constant for the line shape.[22] Here, $B_\Delta = (1/2)B_{1/2}$ is the half-width at half-maximum (HWHM), so that $\sigma = B_\Delta/(\ln(2/\pi))^{1/2}$.

In the homotopy technique, the resonant line position at the orientation $(\theta + \delta\theta, \varphi + \delta\varphi)$ as calculated from the knowledge of the line position at the orientation (θ, φ) using the LSF technique and Taylor series expansion is as follows:[26]

$$B_r(i,\theta + \delta\theta,\varphi + \delta\varphi) = \text{iterative limit of}\left[-\left(\frac{\partial^2 S}{\partial B^2}\right)^{-1}_{B_r'}\left(\frac{\partial S}{\partial B}\right)_{B_r'}\right] \tag{4}$$

with

$$S \equiv (|E_{i'} - E_{i''}| - h\nu_c)^2 \tag{5}$$

where h is Planck's constant and one starts the iteration with $B_r' = B_r(i,\theta,\varphi)$. For calculation purposes, the square bracket in eq 4 is expressed as[26]

$$-\left(\frac{\partial^2 S}{\partial B^2}\right)^{-1}\left(\frac{\partial S}{\partial B}\right) = -(|E_{i'} - E_{i''}| - h\nu_c)\,\mathrm{sign}(E_{i'} - E_{i''}) \div \left(\frac{\partial E_{i'}}{\partial B} - \frac{\partial E_{i''}}{\partial B}\right) \tag{6}$$

The required eigenvalues and eigenvectors of the spin-Hamiltonian matrix are computed by the use of the subroutine JACOBI, which diagonalizes real symmetric matrices, and is particularly efficient when the off-diagonal elements in the SH matrix are infinitesimally small, as is naturally the case in homotopy.[27]

The simulated first-derivative absorption spectrum is expressed by exploitation of eq 1 for the Gaussian line shape as

$$F_c(B_k,\nu_c) = \sum_i N|\langle\Phi_{i'}|B_{1x}S_x + B_{1y}S_y + B_{1z}S_z|\Phi_{i''}\rangle|^2 \times \exp[-(B_k - B_{ri})^2/\sigma^2](B_k - B_{ri})/\sigma^2 \tag{7}$$

In eq 7, the constant N may be appropriately chosen, e.g., such that the calculated value with the largest magnitude for all B_k is equal to 1.

For application of the LSF technique to evaluate the SH parameters and the line width, the χ^2 function is defined as the sum of the weighted squares of the differences of the calculated and measured first-derivative absorption signals at the magnetic field values B_k within the range of the magnetic field considered:

$$\chi^2 = \sum_k [F_c(B_k,\nu_c) - F_m(B_k,\nu_c)]^2/\sigma_k^2 \tag{8}$$

where $F_c(B_k,\nu_c)$ and $F_m(B_k,\nu_c)$ are, respectively, the calculated and measured values of the first-derivative EPR signal and σ_k is the weight factor (related to the standard deviation of the datum k).

In the LSF technique, the vector $\mathbf{a^m}$ constituted by the parameters corresponding to the absolute minimum of the χ^2 function is obtained from $\mathbf{a^i}$, the vector constituted by the initially chosen value of SH parameters and line width by the following relation:[28]

$$\mathbf{a^m} = \mathbf{a^i} - (\mathbf{D''}(\mathbf{a^i}))^{-1}\mathbf{D'} \tag{9}$$

In eq 9, $\mathbf{D'}$ is the column vector whose elements are the first derivatives of the χ^2 function with respect to the parameters evaluated at $\mathbf{a^i}$, and $\mathbf{D''}$ is the matrix whose elements are the second derivatives with respect to the parameters evaluated at $\mathbf{a^m}$.

Since $\mathbf{a^m}$ is not initially known, the elements of the matrix $\mathbf{D''}$ are, in practice, evaluated with respect to $\mathbf{a^i}$, referred to as $\mathbf{D''}(\mathbf{a^i})$. A new set of parameters, denoted by the vector $\mathbf{a^f}$, is thus calculated using the right-hand side of eq 9. This calculation is carried out iteratively until a sufficiently small value of the χ^2 function, consistent with experimental uncertainties, is obtained.[22]

Finally, the parameter errors, Δa_j, are estimated statistically using the matrix constituted by the second derivatives of the χ^2 function:[29]

$$\Delta a_j = \epsilon_{jj}^{1/2} \tag{10}$$

where the matrix ϵ is defined as

$$\epsilon = ({}^1/_2\mathbf{D''})^{-1} \tag{11}$$

Acknowledgment. We thank Dr. Keith A. Earle (Cornell University) and Dr. Alex I. Smirnov and Professor R. Linn Belford (Illinois EPR Research Center) for their help in acquiring high-field EPR spectra and Dr. Mark J. Nilges (Illinois EPR Research Center) for helpful discussions. This work was supported by a Research and Professional Development Grant from Gettysburg College, the Undergraduate Research Committee at the University of Evansville, the NIH (Grant No. RR07126), and the NSF (Grant No. CHE9615910). Acknowledgment is made to the donors of the Petroleum Research Fund, administered by the American Chemical Society, for partial support of this research. This work was supported by an award from Research Corporation, and used the resources of the Illinois EPR Research Center (NIH Grant P41-RR01811), an NIH-supported Resource Center.

IC990377+

(26) Misra, S. K.; Vasilopoulos, V. *J. Phys. C: Condens. Matter* **1980**, *13*, 1083.
(27) Press, W. H.; Teukolsky, S. A.; Vetterling, W. T.; Flannery, B. P. *Numerical Recipes in Fortran*; Cambridge University Press: Cambridge, MA, 1992; pp 456−462.
(28) Misra, S. K. *J. Magn. Reson.* **1976**, *23*, 403.
(29) Misra, S. K.; Subramanian, S. *J. Phys. C: Condens. Matter* **1982**, *15*, 7199.